Available online at www.sciencedirect.com

SciVerse ScienceDirect

Ceramics International 38 (2012) 4035–4047

CERAMICS INTERNATIONAL

www.elsevier.com/locate/ceramint

Mechanical behaviour of MgO–C refractory bricks evaluated by stress–strain curves

L. Musante [a], L.F. Martorello [a], P.G. Galliano [a], A.L. Cavalieri [b], A.G. Tomba Martinez [b,*]

[a] Tenaris Siderca R&D (REDE AR), Dr. Simini 250 (2804) Campana, Argentina

[b] Instituto de Investigaciones en Ciencia y Tecnología de Materiales (INTEMA), Fac. de Ingeniería (UNMdP), CONICET, Av. J.B. Justo 4302 (7600) Mar del Plata, Argentina

Received 17 September 2011; received in revised form 21 January 2012; accepted 24 January 2012
Available online 31 January 2012

Abstract

In this work, the mechanical behaviour of a set of resin- and pitch-bonded MgO–C refractories containing metallic additives was evaluated in laboratory tests at high temperature in a non-oxidant atmosphere. Commercial bricks were used for this evaluation, and a comprehensive characterization of the as-received materials was performed using several techniques (mineralogical analysis by X-ray diffraction, density and porosity measurements, differential thermal and thermogravimetric analyses and microstructural analysis by reflected light microscopy coupled with cathodoluminiscence accessory and scanning electron microscopy). Stress–strain curves in compression were obtained at room temperature, 600, 1000 and 1400 °C under flowing N_2 gas. An Instron 8501 servo-hydraulic machine was used with a capacitive extensometer suitable for axial strain measurements at high temperatures. A constant displacement of 0.1 mm/min was applied until specimen failure. Several parameters were calculated from the stress–strain curves: failure stress, failure strain, yield stress and secant Young's modulus. Moreover, a comprehensive characterization of the tested specimens was carried out. The analysis of the mechanical behaviour has been based on previous research and the results have been interpreted in terms of the thermal evolution of the brick's microstructure. The resin-based refractory exhibited the higher values of mechanical strength and Young's modulus in the entire range of testing temperatures. Up to 1000 °C, the mechanical behaviour was controlled by the type of binder and the changes in porosity whereas at 1400 °C, the main differences between the responses of resin- and pitch-based refractories were mainly caused by the metallic additive reactions.

Keywords: C. Mechanical properties; E. Refractories

1. Introduction

MgO–C refractory bricks are the most widely used materials for the working lining of steelmaking vessels such as electric furnaces, converters and ladles [1–5]. These materials withstand a broad range of temperatures under operation, from room temperature to 1600–1700 °C, and undergo severe thermal cycles. Material properties are variable and depend not only on the original design but also on the microstructural and chemical changes produced by the thermal conditions of the system.

Much effort has been made to improve the performance of MgO–C bricks. Initially, this effort was mainly empirical in nature, but fortunately it became more rational as a result of much basic and technological research. In spite of the solid background knowledge concerning the main factors governing the chemical, mechanical and thermomechanical wear of MgO–C refractories, investigation into this type of material are still of interest to manufacturers and consumers industries. Environmental impact reduction and the use of nanotechnology, among others demands, combined with high in-service performance, are requirements that have become more important and have to be equally satisfied.

The mechanical properties of MgO–C bricks, with and without antioxidants, have been dealt with extensively in the past [6–21]. However, little research has studied the mechanical behaviour (not only mechanical properties data) together with

* Corresponding author at: Av. Juan B. Justo 4302 (7600) Mar del Plata, Argentina. Tel.: +54 223 4816600; fax: +54 223 4810046.
E-mail address: agtomba@fi.mdp.edu.ar (A.G. Tomba Martinez).

0272-8842/$36.00
doi:10.1016/j.ceramint.2012.01.062

deformation and fracture mechanisms. The flexibility given by graphite and the influence of the microstructural evolution by reactions within the refractory components (carbonization of the organic binder, direct oxidation of graphite, carbothermal reduction of magnesia, formation of carbides, nitrides or oxides from metallic antioxidants, spinelization, etc.) are well established facts. According to the main contributions in the study of deformation and rupture mechanisms [6–9,11,12,14–16], the mechanical behaviour of MgO–C refractory bricks in the midrange of temperature (RT-1000 °C) is determined by change in the porosity/cracks due to the carbonization of the organic binder (pitch or resin) and the loss of graphite. Both processes decrease the mechanical performance. Above 1000 °C, there is a difference between the presence and the absence of antioxidant additives in the refractory composition; the most commonly studied additives have been Al and Si. These agents react with other components to form new phases such as Al_4C_3, SiC and $MgO{\cdot}Al_2O_3$, which could contribute to enhance the mechanical response (besides the inhibition of graphite oxidation) up to 1400–1500 °C, the maximum temperature currently used in the mechanical evaluation [18]. The effect of these new phases on the mechanical strength of aluminum-containing MgO–C materials (2.5 and 5.0 wt.%) using argon flow has been discussed in the literature [9,15,16,18]. The strengthening by Al_4C_3 formed in the range of 1000–1500 °C has been recognized and attributed to the plate or skeletal shape of the carbide particles. With respect to spinel, Baudín et al. [15] found an increase in the modulus of rupture between 1200 and 1450 °C, which was related to the sealing effect of spinel particles. Taffin et al. [9] also recognized an increase in this parameter between 1300 and 1500 °C, but they attributed it to the more compact lattice of spinel compared with carbide. The effect of silicon has been less analysed. Taffin et al. [9] have mentioned that no mechanical improvement of mechanical properties of silicon-containing MgO–C materials was observed although the range of temperature was not specified. This fact was attributed to the formation of forsterite ($2MgO{\cdot}SiO_2$) besides the SiC (that begins at 1300 °C), which could enhance the mechanical properties itself. In the midrange of temperatures (below 1300 °C), the formation of SiO_2 and silica glass would also occur, which may also be favourable due to a local filling of the structure [9]. The sealing effect of the dense magnesia zone could also contribute to the increase in the mechanical strength [15–18].

The reaction mechanism for the formation of new phases (solid–solid, liquid–solid or gas–solid), which is strongly affected not only by the temperature but also by the atmospheric composition, is very important in defining the characteristics of the new phases (morphology, location) and determining its influence on the mechanical properties. As a consequence, the mechanical properties strongly depend on the temperature and also on the composition of the surrounding atmosphere.

Even if a great part of previous research has been related to industry demands, the evaluation of as-received commercial bricks is infrequent due to the difficulties associated with the lack of control over the composition and the variability associated with commercial products. However, this approach has the advantage of determining the actual properties of the material to be used in the plant and allows more reliable extrapolation to actual service conditions. In this work, the mechanical behaviour of a set of resin- and pitch-bonded MgO–C refractories containing metallic additives was evaluated in laboratory tests from room temperature to 1400 °C in an N_2 atmosphere. These refractories have been used in Tenaris steelshops as working lining materials in both electric arc furnaces and ladles. A comprehensive characterization of the as-received and tested materials was performed using several techniques. The analysis of the mechanical behaviour has been based on previous research and the results have been interpreted in terms of the thermal evolution of the brick's microstructure.

2. Experimental

Three types of MgO–C commercial bricks (produced by the same manufacturer) currently used in the steel industry, labelled A1, A2 and B, were evaluated. According to their technical data sheets, these materials have two different carbon binders, – pitch (materials A1 and A2) and resin (material B) – different contents of sinter (S) and electrofused (EF) MgO aggregates, as shown in Table 1.

2.1. Materials characterization

The as-received bricks were characterized by several techniques. Powder samples representative of the whole refractory bricks were prepared by crushing, quartering and grinding. The mineralogical analysis was carried out on powdered samples (<70 mesh) by X-ray diffraction (XRD; Philips) using Co Kα radiation at 40 kV and 30 mA with an Ni filter. The Rietveld method was employed for quantitative analysis (FullProf software). The bulk density (ρ_b) and the

Table 1
Characterization of as-received MgO–C refractories.

	A1		A2		B	
C-bond	Pitch				Resin	
S:EF[a]	0.75:0.25		0.25:0.75		0.10:0.90	
Main phases	MgO (periclase): 92 wt.% C (graphite): 5–6 wt.%		MgO (periclase): 93–94 wt.% C (graphite): 4–5 wt.%		MgO (periclase): 93–94 wt.% C (graphite): 6–7 wt.%	
Minor phases	Al: 2–4 wt.%		Al: 2–4 wt.%		Al–Mg, Si: 3–4 wt.%	
ρ_b (g/cm^3)	3.00 ± 0.01		3.00 ± 0.01		2.98 ± 0.01	
ρ_{pyc} (g/cm^3)	3.15 ± 0.02		3.18 ± 0.03		3.17 ± 0.04	
π_a (%)	3.9 ± 0.2		4.6 ± 0.1		3.5 ± 0.1	
π_t (%)	4.8 ± 0.2		5.7 ± 0.2		5.8 ± 0.3	
π_c (%)	0.9 ± 0.2		1.1 ± 0.2		2.3 ± 0.3	
T^{DTA} (°C)	530 610	932	530 610	938	392	890
Δm^{TGA} (%)	4.8	8.2	4.2	7.8	2.0	10.0

[a] S:EF: sintered magnesia (S) to electrofused magnesia (EF) ratio estimated from microscopic analysis.

apparent porosity (π_a) were determined based on the DIN EN 993-1(DIN 51056) standard [22]. The pycnometric density (ρ_{pyc}) was measured on powdered samples (<70 mesh) employing kerosene in accordance with an internal method based on the ASTM C329-88 standard [23]. The true porosity (π_t) and the closed porosity (π_c) were calculated using the following relationships: $\pi_t = (1 - \rho_b/\rho_{yc}) \times 100$ and $\pi_c = \pi_t - \pi_a$. The thermal differential (DTA; Shimadzu DTA-50) and thermogravimetric (TGA; Shimadzu TGA-50) analyses were performed on powdered samples (<70 mesh) up to 1400 °C (10 °C/min) in air. Platinum cups (6 mm in diameter and 2 mm in height) were used for holding the samples in both thermal analyses; samples between 24–30 mg and 12–16 mg were analysed by DTA and TGA, respectively. The amounts of the organic binder and graphite were estimated from the TGA data. The microstructure of the bricks was observed by: (a) scanning electron microscopy (SEM; Philips XL30) coupled with elementary analysis using an EDAX (energy dispersion spectroscopy by X-Ray) detecting unit and (b) reflected light microscopy (RL; Nikon Labophot2.Pol with Optronics 3CCD video system model DEI 750) coupled with a cathodoluminescence accessory (CL; Cambridge Image Technology Ltd., model 8200 Mk3). The surfaces for observation were obtained by the transversal cutting of cylinders previously embedded in resin to avoid the crumbling of the specimen, and polishing with SiC papers (320 grit) using kerosene as a lubricant/coolant.

2.2. Mechanical tests

Stress–strain curves were determined by applying uniaxial compression [24] using a universal servohydraulic testing machine (Instron 8501) with a high stiffness framework and high density mullite/alumina push-rods (60 mm in diameter). The compressive load was applied parallel to the cylinder axis and alumina disks were placed between the testing specimens and the push-rods. The mechanical tests were carried out at room temperature (RT), 600, 1000 and 1400 °C (heating rate of 5 °C/min), using an electrical furnace (SFL) with $MoSi_2$ heating elements. Before applying the mechanical load, the specimen was kept for 20 min at the testing temperature; after the application of mechanical load, the specimen was free cooled (around 10 °C/min) in the furnace chamber. A continuous flow (5 l/min) of nitrogen gas (99.995%) was used to generate a non-oxidant atmosphere during the heating, the application of mechanical load and the cooling up to 300 °C.

The testing specimens (cylinders of 27 mm in diameter and 40 mm in height) were obtained from the bricks by drilling and machining with diamond tools; the cylinder axis was parallel to the direction of the main compressive loading on the in-service bricks. The change in the specimen height (from which the deformation was calculated) was measured by contact extensometry using a capacitive extensometer (±0.6 μm; 25 mm of gauge length) with SiC knives suitable for high temperature measurements. The tests were carried out in displacement (of the actuator) control with a constant rate of 0.1 mm/min until specimen failure.

The mechanical behaviour characteristics of each material were analysed from the stress–strain curves and the following mechanical parameters were determined: Young's modulus (E), yield stress (σ_Y), mechanical strength (σ_R), and fracture strain (ε_R). The secant Young's modulus was determined at 0.001 of strain. The value of σ_Y was considered as the stress where the curve deviates from linearity by 0.5%; this parameter is not commonly analysed in the literature for these types of materials. The ratio σ_Y/σ_R (in percentage) was considered as a measure of the deviation from the linear elastic behaviour by inelasticity (due to microcracking, for example) or plasticity (due to viscous flow, for instance). Mechanical strength was taken as the maximum stress displayed in the stress–strain curve, which is a common criterion used in these types of materials. The strain corresponding to this condition was taken as ε_R.

The main fracture paths were also analysed by visual inspection. The microstructural changes that occurred in the materials during the high temperature mechanical tests were evaluated using several techniques: mineralogical analysis by XRD, DTA/TGA, density and porosity measurements, and observation by SEM/EDAX. The same methodologies used for the as-received materials were employed. These data are complementary to the information obtained from the mechanical testing and make possible to analyse the main factors determining the mechanical behaviour and the deformation and fracture mechanisms.

3. Results

3.1. Materials characterization

Table 1 shows some of the results obtained from the different characterization techniques used for the as-received refractories.

MgO as periclase and C as graphite were determined to be the main crystalline phases in every material, in addition to small amounts of Al. The presence of Si as a metallic additive was also identified in material B. Taking into account the experimental error of the Rietveld method (±5 wt.%) and the microstructural analysis, the content of this metal (≈1 wt.%) was determined to be lower than that of the aluminium additive.

The microstructural evaluation of A1, A2 and B by SEM/EDS (Fig. 1) confirmed the results of the XRD analysis and the information from the technical data sheets. Electrofused (EF) and sintered (S) magnesia aggregates were observed in the three refractories, together with small Al particles and graphite flakes (G). The images obtained by RL/CL observation (Fig. 2) showed similar characteristics and revealed the presence of Al–Mg alloy and Si metal particles, in a smaller amount, in the B material. The sintered MgO (S) was mainly identified in the fine and medium fraction of MgO particles in the A1 and A2 refractories. Higher amounts of electrofused MgO was detected in the resin-bonded refractory (B), in accordance with the technical data sheet.

No significant differences were observed between the pycnometric densities of the three refractories due to the

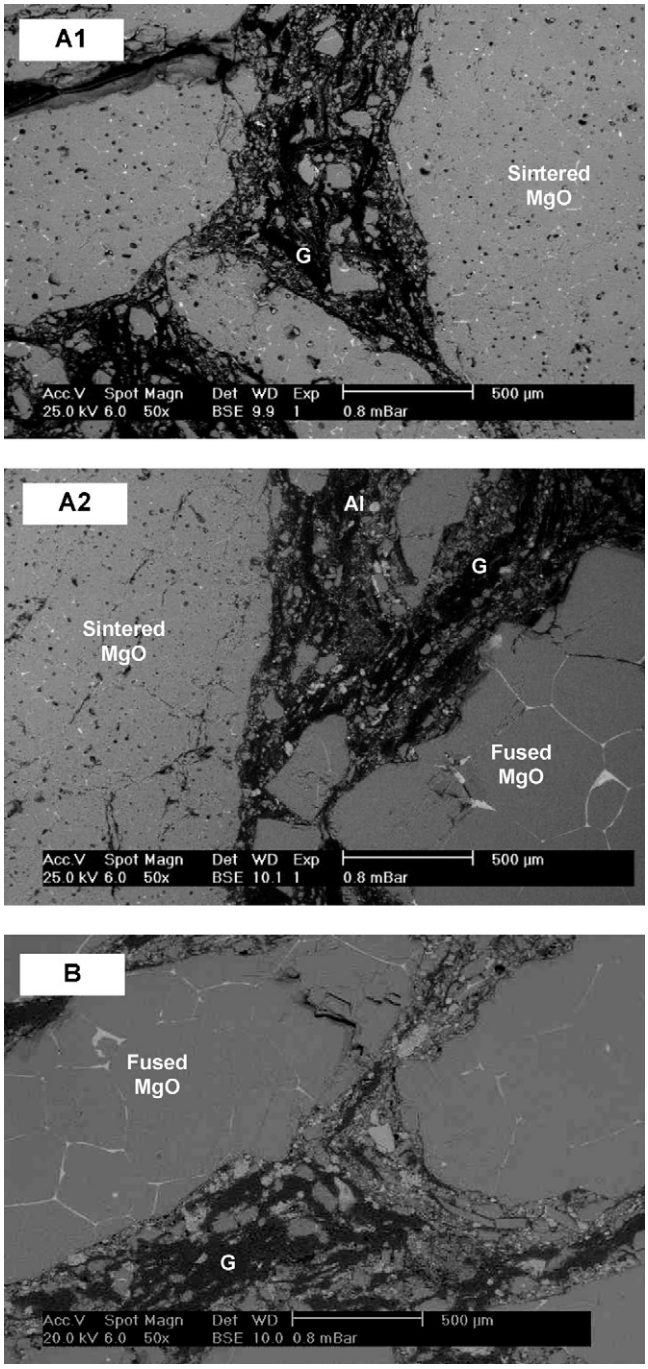

Fig. 1. SEM images of as-received MgO–C refractories.

similarities in their mineralogical composition. Differences between 10 and 30% were observed in the open and true porosities of the different bricks (except the values of π_t for A2 and B, which were very similar). The highest volume fraction of closed porosity was determined for the B refractory, which is consistent with the lowest bulk density; however, this material also has the lowest π_a.

DTA graphs of pitch-bonded materials A1 and A2 (Fig. 3) were very similar with regard to position (temperature) and intensity of peaks. The position of the exothermic peaks identified by DTA (T^{DTA}), in which weight loss was also registered in the thermogravimetric analysis (Δm^{TGA}), is shown in Table 1. The weight loss at temperatures below 650 °C was attributed to the pitch transformations. This was due to the evaporation and thermal scission of volatile species, including a fluid stage in which a mesophase is formed as a precursor to a graphitizable structure or semi-coke [25,26]. A small peak near 400 °C was associated with the mesophase formation (with a little weight loss, <1 wt.%) and another peak occurred at 530 °C with the transformation to semi-coke. The following peak at 610 °C was related to the evolution of volatile matter accompanying the semi-coke phase [25].

DTA thermograms of A1 and A2 also exhibited an endothermic peak around 660 °C due to the melting of the aluminium added as an antioxidant. The weight loss displayed at a temperature slightly higher than 930 °C was attributed to graphite oxidation. At temperatures over 1000 °C, peaks with low definition could be attributed to the several reactions that occur at this high temperature range [9,18,27,28]: (a) liquid Al reacts with the more reactive C coming from the organic binder or with graphite, thus yielding Al_4C_3; the carbide reacts with CO coming from the graphite oxidation, thus producing Al_2O_3 at $T > 1100$ °C; (b) formation of $MgO{\cdot}Al_2O_3$ by the reaction of liquid Al and/or Al_4C_3 with MgO(s) and/or Al_2O_3 with Mg (g) produced by carbothermal reduction of magnesia.

In the B material, different peaks were displayed in the DTA/TGA plots (Fig. 3). DTA exothermic peaks below 600 °C were attributed to resin transformations (condensation, oxidation, dehydration and decomposition reactions [25,26,29]). As reported in the literature [25,30], the weight loss occurred at lower temperatures in resin-based material compared to pitch-based material.

A very small endothermic peak at 656 °C was attributed to the melting of Al alloy (the temperature is lower than the melting point of aluminium due to the presence of Mg as the alloying metal). The weight loss displayed at 800 °C (exothermic peak) was attributed to graphite oxidation. At higher temperatures, low intensity peaks were observed and attributed to the same reactions mentioned above for pitch bonded materials. Moreover, the reactions of silicon have also to be accounted for [9,27]: at $T \sim 1100$ °C, SiO_2 is formed by the reaction of Si with the O_2 of the air. At higher temperatures, SiO_2 transforms to SiC by reaction with C.

Based on the similarity between the DTA thermograms of A1 and A2, it could be assumed that in both materials, the pitch and the graphite flakes have similar qualities (both materials are provided by the same supplier). Since the TGA steps (Fig. 3) corresponding to the carbonization of resin and graphite oxidation were separated in every material (as has been previously reported [26,31]), the content of both components can be estimated from Δm^{TGA} values of Table 1 at temperatures lower than 650 °C and around 900 °C, respectively. Therefore, the contents of the organic binder and the graphite were slightly higher in A1 (4.8 and 8.2 wt.%, respectively) than in A2 (4.2 and 7.8, respectively). The difference seen in the XRD quantitative analysis was attributed to the Rietveld method error (±5 wt.%) together with the incidence of the flakes' orientation on the intensity of the diffraction peaks. On the other hand, the content of the organic binder estimated from the

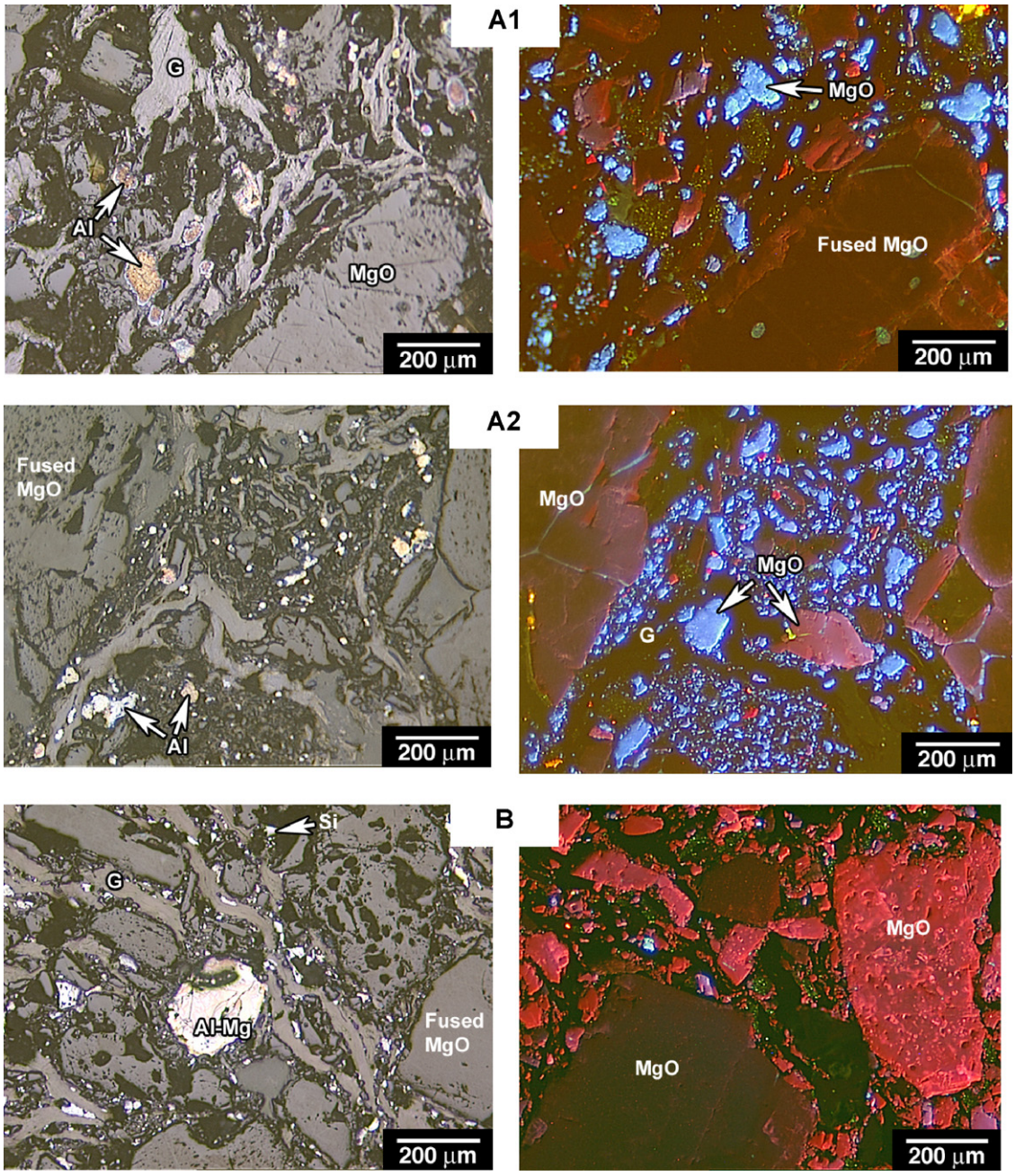

Fig. 2. CL images of as-received MgO–C refractories.

TGA is lower in the B refractory (2 wt.%) and the amount of graphite is higher (10 wt.%) than in pitch-based materials.

3.2. Stress–strain curves

Fig. 4 shows the compressive stress–strain curves for materials A1, A2 and B at the different testing temperatures. The mean values of the mechanical parameters obtained from these curves are plotted in Fig. 5 as a function of the testing temperature. The relative experimental error of the mechanical parameters measured by the stress–strain methodology used here are smaller than 20% and 25% of the mean value of the mechanical resistance and secant Young's modulus, respectively [24].

The three materials exhibited a quasi-brittle behaviour within the range of the testing temperatures since a deviation from the linear behaviour is observed in every case. The lower values of σ_Y/σ_R at 600 and 1000 °C (Fig. 5) indicate that this behaviour is more marked for the three materials at these temperatures; the non-linear response is slightly higher at RT than at 1400 °C. A softening behaviour was also observed in A1 and A2 at all of the testing temperatures (Fig. 4); in general, it was more noticeable at 600 °C.

The values of the Young's modulus and the fracture strength were in the order of those reported in the literature for refractories with similar compositions [7–9,13,15–17]. The elastic modulus and the mechanical strength of B were higher than the values of A1 and A2 in every testing condition. In

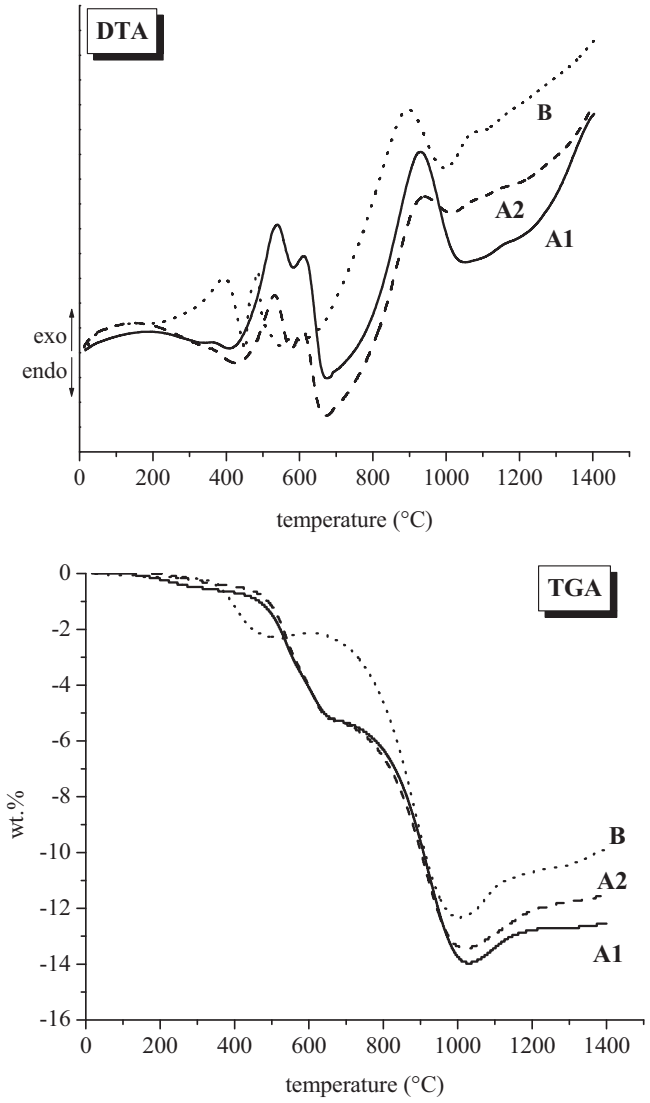

Fig. 3. DTA and TGA thermograms of as-received MgO–C refractories.

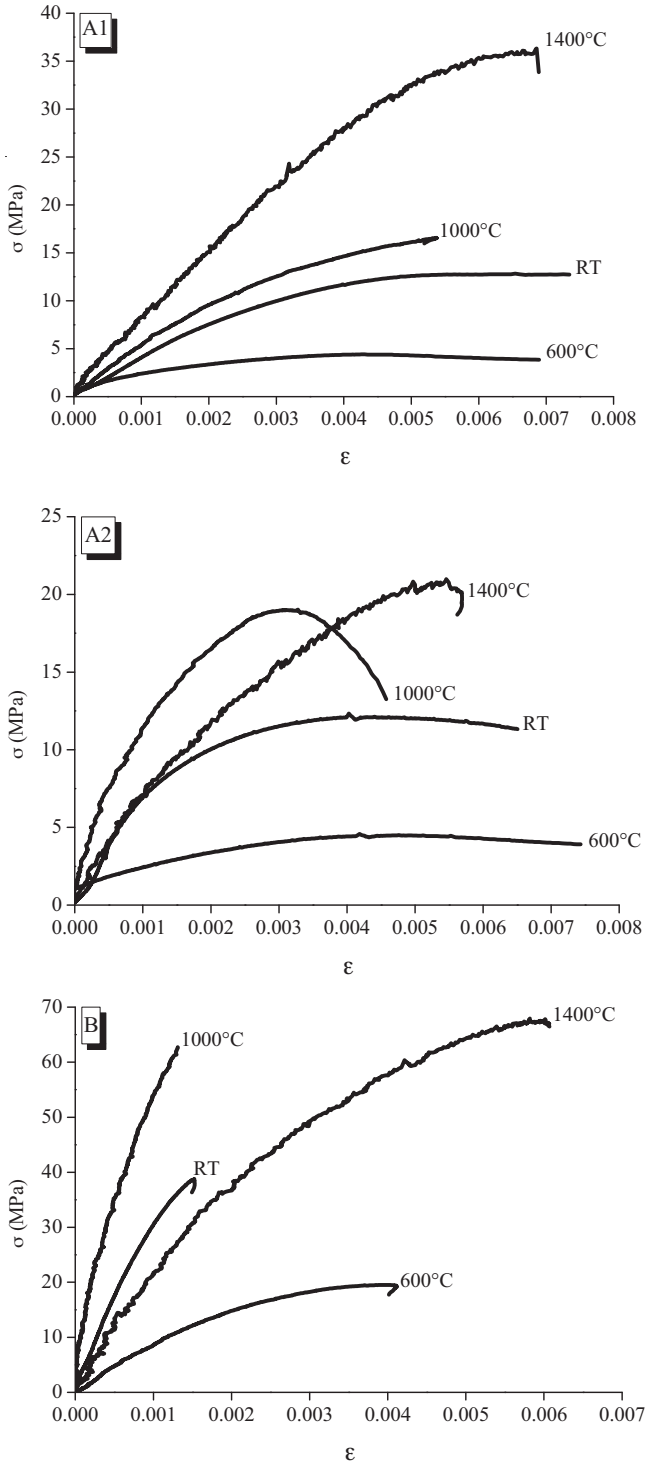

Fig. 4. Stress–strain curves of MgO–C refractories.

relation with these facts, the fracture strain values were in general lower for the resin-bonded refractory. Both pitch-based materials showed very similar mechanical responses.

Regarding the thermal dependency of mechanical properties, there was a significant reduction from RT to 600 °C and a full recovery at higher temperatures. The changes between 1000 and 1400 °C have been associated primarily with the presence of metallic additives [9,15,16,18]; these changes were dependent on the specific tested material. The variation in fracture strain in relation to the testing temperature was different between the resin-bonded refractories and the pitch-bonded refractories.

In each case, the fracture ran mainly in a diagonal direction across the cylinder (Fig. 6), as is characteristic of compression tests where friction effects act in the contact area between the flat surfaces of the specimens and the push-rods (or the disk between them). In some cases, other cracks also formed near the load-bearing surfaces of the cylinders (Fig. 6b). In several cases, the cracks propagated mainly through the bonding phase surrounding the aggregates (Fig. 6c); however, the fracture of aggregates was also observed but less frequently. At 1000 and 1400 °C the specimens showed a superficial discolouration due to graphite oxidation (Fig. 6b and c), which was more noticeable at this last temperature. In agreement with the more pronounced softening behaviour, a high number of cracks were observed in A1 and A2 at 600 and 1000 °C; at 1400 °C, material B also exhibited a high density of cracks.

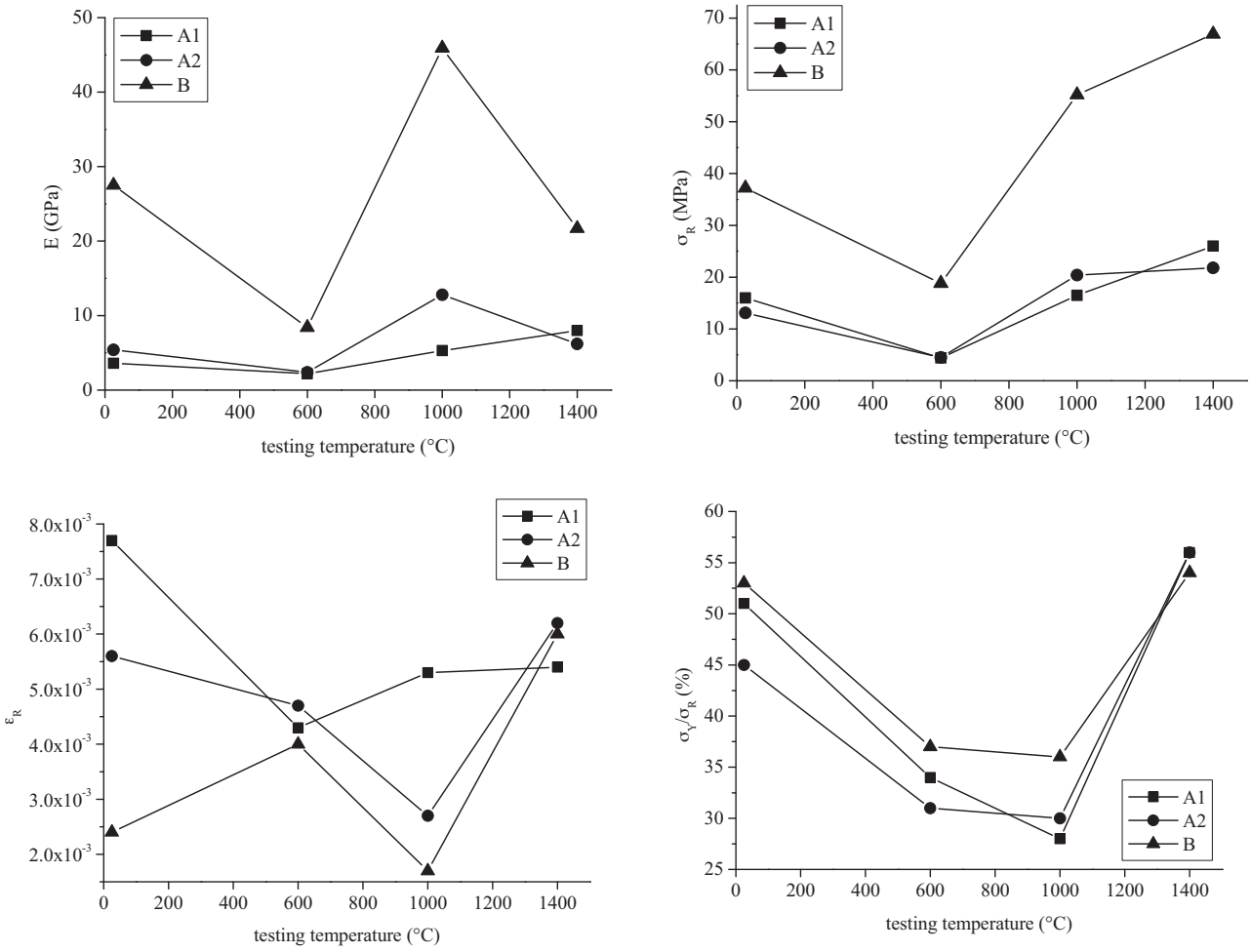

Fig. 5. Variation of mechanical parameters as a function of testing temperature.

3.3. Post-testing characterization

In the three materials, an increase in the baseline intensity of XRD patterns was observed in the region of the principal peak of graphite (30.7° 2θ, File No. 01-0640) at 600 °C and 1000 °C. This increase was attributed to the contribution made by the structures formed by the thermal transformation of the organic binder, which has a certain degree of structural ordering [25,32]. Similar XRD patterns were observed in the A1 and A2 materials at the different testing temperatures, as was also the case with the as-received samples. Only very weak peaks of new phases (AlN, Al_4C_3 and spinel) were identified in these pitch-bonded materials at 1000 and 1400 °C; at these temperatures, the changes in the XRD pattern of mechanically tested specimens of B were more noticeable.

At the highest temperatures, a small peak around 38.7° 2θ, more clearly defined at 1000 °C, was attributed to the presence of AlN (File No. 75-1620) due to the reaction between the Al (or Al_4C_3, which can be formed even in the presence of N_2 depending on the oxygen partial pressure [33]) and the N_2 from the furnace atmosphere [33,34]. At 1400 °C, B showed a very small peak around 37.1° 2θ that could be associated with the formation of Al_4C_3 (File No. 79-1736),which has been observed at this temperature even in nitrogen [15]. Moreover, peaks assigned to Al (File No. 03-0932) and graphite (File No. 01-0640) were present even at 1400 °C in all of the materials.

The presence of spinel ($MgO{\cdot}Al_2O_3$) coming from the reaction of MgO with Al (gas or liquid), Al_2O_3 or Al_4C_3 in the specimens tested at high temperature is difficult to detect due to the overlapping of its principal peaks with those of MgO and Al. However, in A1 tested at 1400 °C, peaks assignable to spinel (File No. 82-2424) were more clearly identified with respect to the other materials. In the resin-bonded refractory, peaks corresponding to silicon disappeared just at 1400 °C, where small peaks of SiC were identified (Files No. 27-1402 and 73-2086, respectively).

DTA thermograms of tested specimens showed peaks corresponding to pitch or resin transformations similar to those of the as-received materials, but with slight differences in position (temperature) and lower intensity; this suggests that the carbonization of the organic binders during the heating and the time spent at high temperature was incomplete even at 1400 °C. Pitch and resin organic binders decompose by complex mechanisms at a wide range of temperatures [25]. In conditions suitable for ensuring a complete transformation and a high coke yield, the evolution of gases occurs up to temperatures near 1000 °C, and even at higher temperatures the structural changes in the carbon continue [25]. The transformation of the organic

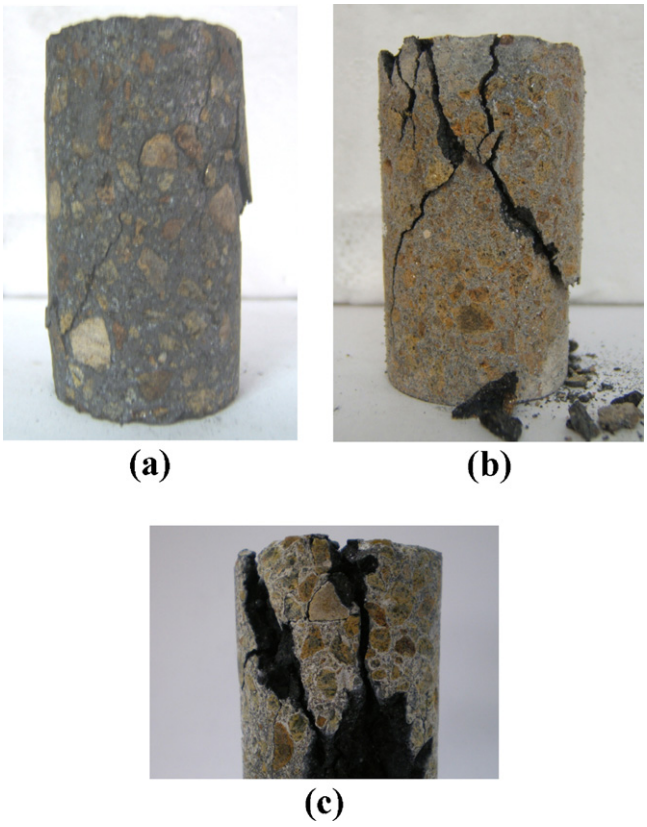

Fig. 6. Fractured specimens: (a) A1, RT; (b) B, 1000 °C; (c) A2, 1400 °C.

binders could not be completed during the mechanical test under nitrogen flow due to several reasons: (a) the heating rate could be not slowed enough to complete the processes, (b) the existence of a thermal gradient within the specimens, mainly during the heating, due to its limited thermal conductivity, (c) the low catalytic effect of the oxygen [25] as a consequence of its low partial pressure within the specimen (nitrogen flow displaces and dilutes oxygen in the area around specimen [24]), and (d) the closeness between the high testing temperatures and the temperature at which the transformation stops.

The inhibition of graphite oxidation by using N_2 atmosphere (by displacement and dilution effects) was also inferred from the reduction of the TGA step at around 850–950 °C with respect to the steps of the as-received refractories; however, graphite loss occurred to a certain degree (see the discoloured surface of the specimens in Fig. 6b and c). The analysis of the TGA thermograms of the tested specimens was difficult to perform due to several reactions occurring simultaneously, mainly at the highest temperature, with some of them leading to weight increase and others to weight loss. However, the results confirmed the conclusions inferred from DTA regarding the incomplete process of the carbonization of the organic binder and the reduction of graphite oxidation.

In Fig. 7, the mean values of density and porosity as a function of the testing temperatures are plotted. The values at 1400 °C are considered only as estimations as they have a large associated experimental error (around 10%). Except for the formation of spinel ($MgO{\cdot}Al_2O_3$) due to a reaction of MgO, the rest of the processes occurring at high temperatures lead to an increase of the solid density which is the general trend observed in the A2 and B materials. Even considering the experimental error, a more considerable change was observed at 1400 °C, in agreement with the identification of new phases by XRD. In the case of B and A2, the formation of phases with higher pycnometric densities (for instances, SiC replacing Si in B) prevails. However, the value of ρ_{pyc} for A1 went down from 1000 °C to 1400 °C; this fact is attributed primarily to spinel formation, as was inferred from the XRD analysis of tested specimens.

On the other hand, for the three refractory materials, the apparent density decreased as the testing temperature increased. Considering the overall increase of ρ_{pyc}, this behaviour indicates an increase in the true porosity, as displayed in the corresponding plot (Fig. 7), which is more considerable in B after testing at 1400 °C. The total porosity increase is mainly associated with the transformation of organic binders (open and closed pores and cracks) [25,26] and the partial oxidation of the residual carbon and graphite. Other processes such as the oxide-impurity reduction, the spinel and Al_4C_3 formation and the carbothermal reduction of MgO can also be accompanied by an increase in porosity [15,18]. Carbothermal reduction of MgO at temperatures lower than 1400 °C has been reported [15]. Moreover, the formation of Mg (g) due to the presence of metallic antioxidant additives such as Al, Si, Mg or alloys in the brick composition lowers the formation temperature and/or the partial pressure of Mg (g) by metallic vaporization and metallothermic reduction [27,35]. These processes also contribute to increasing the porosity unless the magnesium re-oxidizes, thus forming a dense layer.

The apparent porosity increased with the testing temperature, as has been reported frequently in the literature, whereas the closed porosity exhibited different behaviour. The changes in π_a of both pitch-bonded materials were very similar, and distinct to those undergone by B. Based on this fact and bearing in mind the differences in the refractories' composition, the variation in open porosity is mainly attributed to changes in the organic binder. The smaller change in the apparent porosity of A1 and A2 with respect to B could also be attributed to the sintering of fine particles of MgO [36] during the heating and time spent at temperatures $\geq$1000 °C in the mechanical tests; the presence of a higher amount of sintered magnesia (with a higher impurity level in medium and fine grains than those present in electrofused magnesia [37,38]) in A1 and A2 could favour the sintering process [36]. The evolution of the volumetric fraction of closed pores is very similar between the three materials up to 1000 °C. The decrease of π_c from 600 to 1000 °C comes from the opening of closed pores when volatiles were evolved, leading to an increase in the apparent porosity. In the resin bonded material, the subsequent increase in closed porosity is partially due to transformation of open micropores into closed micropores [25]; this process does not occur in the pitch binder. Moreover, the final graphitizable structure has a lower amount of macropores whereas the non-graphitizable carbon coming from resin has a high amount of micropores [25,26]. The increment of closed porosity could also be attributed to the filling of open pores by crystals from the new phases.

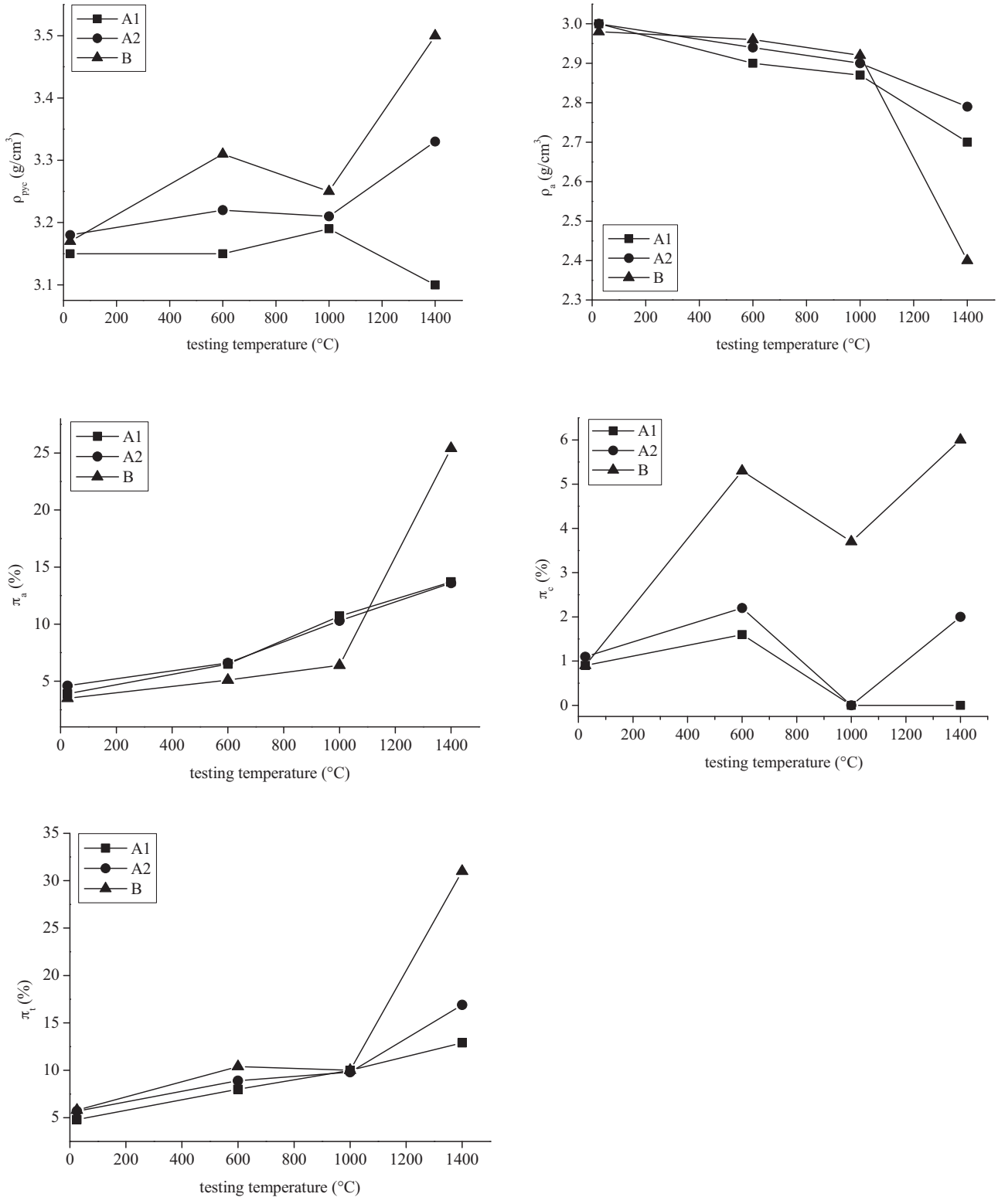

Fig. 7. Density and porosity of tested specimens as a function of testing temperature.

The results obtained from the observation of tested specimens by SEM agree with the XRD and DTA/TGA data. The specimens tested at 600 °C and 1000 °C did not show noticeable changes in the refractories' microstructures. In Fig. 8, the micrographs of specimens tested at 1400 °C are shown. In A1, A2 and B, metallic additives were already identified at this temperature, as has been reported by other authors [14]; in B, the Al and Si particles had a melted aspect. Moreover, some features associated with spinel according to the literature [28] and the EDS analysis were identified in both pitch-based refractories. Furthermore, the morphology of this spinel is indicative of its formation from the metallic aluminum [28]. In B,

another type of microstructural feature was observed (Fig. 8), in which different proportions of MgO, Al_2O_3 and SiO_2 were detected by EDS. Neither a clear identification of crystalline phases nor the presence of spinel in these regions could be achieved. Based on their composition, it is supposed that these phases came from the original silicon, SiO_2 or SiC. The presence of glassy phases in these regions was not discarded [9].

In summary, from the analysis of all the post-testing characterization, we conclude that several changes occurred during the mechanical testing at high temperature:

- the incomplete carbonization of the binder and the inhibition (although incomplete) of direct graphite oxidation from 600 to 1400 °C,
- the formation of new phases coming from reactions involving the metallic additives, but different depending on whether the specimen was a pitch-bonded or resin-bonded refractory; the reactions involving the metallic aluminum were incomplete,
- the increase of the apparent and total porosities up to 1400 °C.

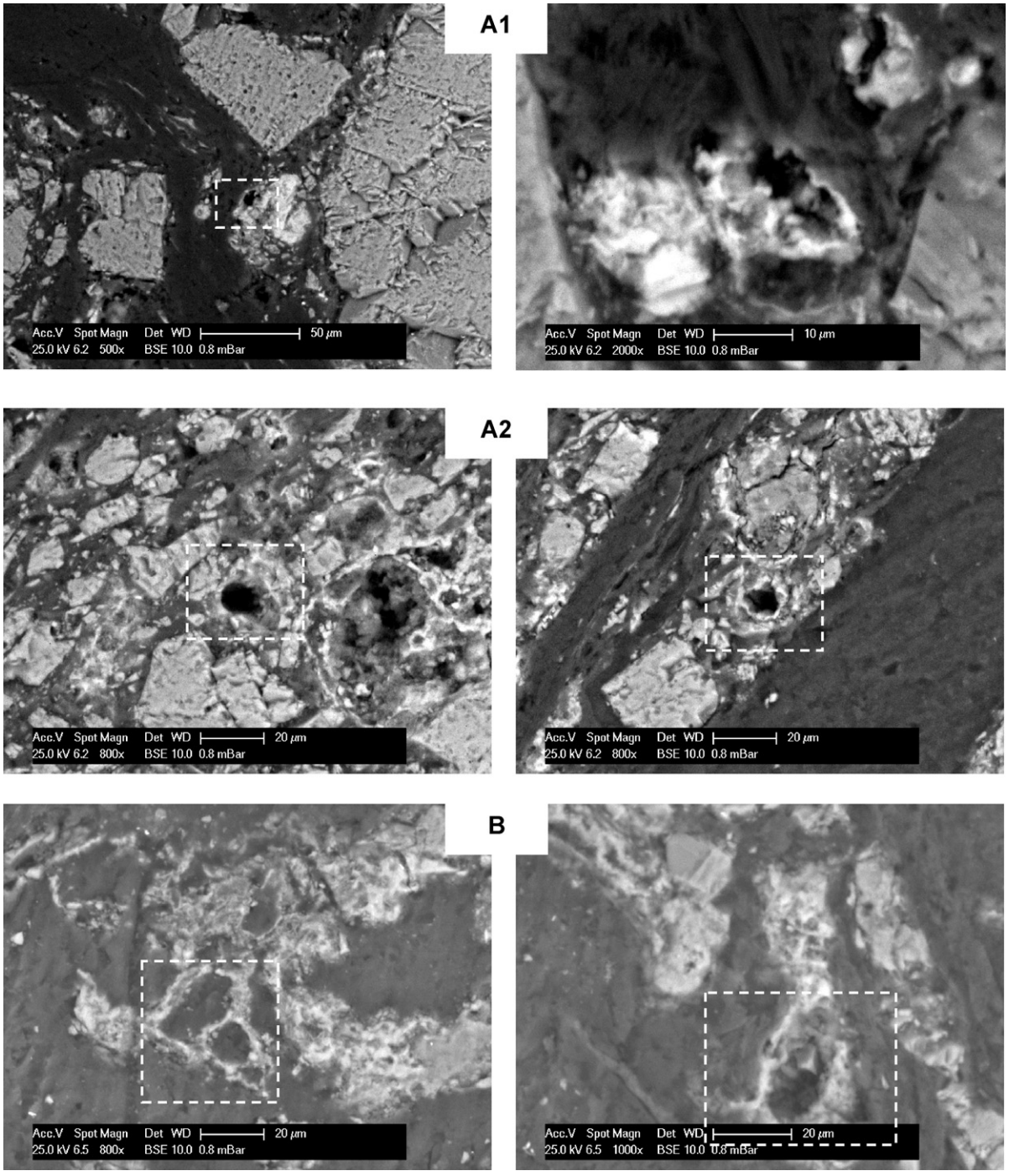

Fig. 8. SEM images of MgO–C specimens tested at 1400 °C.

4. Discussion

The differences in the mechanical behaviour between the tested materials are mainly associated with differences in brick matrices, since it is the weakest mechanical link in the brick's structure in all of the testing conditions. Moreover, the main chemical and microstructural changes at high temperatures occur in the bonding phase (organic binders, metallic additives and fines of MgO). Considering the crack path of broken specimens (Fig. 6), the defects acting as critical flaws are probably pores and cracks already present in the matrix. When the mechanical test is performed at high temperature, the cracks also come from the thermal expansion mismatch between the different components of the refractory. The closure of cracks could also occur as well as pore filling, bridging or strengthening produced by the new phases.

At RT, the values of the mechanical properties of both pitch-bonded refractories are very similar due to similarities in brick composition. On the other hand, the higher Young's modulus of B compared to that of A1 and A2 materials, as well as the more marked softening behaviour of the latter, are mainly determined by the C-bond type: resin binder vs. pitch binder. The higher stiffness of resin and resin-bonded bricks has been already recognised [39,40] although the opposite tendency was also reported for MgO–C refractories [13,17]. Similar considerations explain the higher mechanical strength of this material [32,39,40]; however, other authors also reported higher mechanical strength for pitch-bonded MgO–C refractories [13,17,41].

The fracture strain of the three materials at RT is rather higher than the value estimated by the σ_R/E ratio due to their non-linear behaviour. This non-linearity could be attributed to several mechanisms of irreversible deformation [8,13,17]: propagation of pre-existing cracks and pores and those generated during the mechanical tests (microcracking), shearing or crumpling of graphite and plastic deformation of the organic binders. The value of ε_R for B was lower than the values for A1 and A2; in consequence, B has the lowest ability to accommodate stress. The presence of resin, which has less flexibility than pitch [32], determines B's ability to deform much more than graphite content at room temperature.

At 600 °C, the mechanical properties deteriorated for the three refractories. The effect is more pronounced in the Young's modulus of B (E threefold decrease) and in the fracture strength of pitch bonded materials (σ_R decreases almost fourfold). This mechanical degradation is due to the organic binder transformation, as has been extensively reported in the literature [6,7,13–15]. At this temperature, an increase in total porosity (about 50% in every material, by pores and cracks) takes place that reduces the stiffness and the mechanical strength of materials. Moreover, semi-coke and a highly disordered glassy-carbon phase are formed in pitch- and resin-bonded refractories, respectively [25]; little documentation exists regarding the sole effect of these structural changes on the mechanical properties of the materials (a reduction in the mechanical strength of the resin after thermal treatment at around 600 °C has been reported [42], but the values were calculated including pores and cracks). In the case of pitch, it should be expected that its transformation to semi-coke should increase stiffness with respect to the original pitch whereas the opposite would occur when the stiffer resin becomes a highly disordered glassy-carbon; if this is the case, it could be the reason for the greater variation of the Young's modulus in B.

On the other hand, the transformation of all binders up to 600 °C leads to an increase in the non-linear behaviour in every material, which is mainly attributed to an increase in microcracking due to the generation of pores and cracks; this mechanism intensifies the softening behaviour in A1 and A2. However, the ability to deform is lessened in the pitch-bonded refractories (lower ε_R) and increased in B. The dominant effects are the decrease in the fracture strength in the pitch-bonded refractories and of the Young's modulus in the resin-bonded refractory. In agreement with the higher σ_Y/σ_R ratio, the deviation between the estimated and experimental fracture strains was greater than at RT. Even when differences between the three refractories in the ability to deform reduce significantly, B remains the least able to accommodate stress.

From 600 °C to 1000 °C, a recovery of the mechanical properties is observed that even exceeds the values at RT. This effect is again more pronounced in the Young's modulus of B and in the fracture strength of A1 and A2. Within this temperature range, the change in porosity is not the controlling factor for the mechanical properties (Fig. 7), but rather the presence of a new phase coming from the metallic antioxidant additives, namely AlN (detected by XRD). Besides the binder or morphology effects, AlN is a stiff and highly resistant phase that increases the Young's modulus and the fracture strength of the whole specimen. One cannot rule out the contribution of Al_4C_3 even though it could not be clearly identified by XRD or SEM at this temperature. The ordering of the glassy carbon phase coming from resin [25] is another factor improving the mechanical parameters.

The variations of fracture strain between 600 °C and 1000 °C are correctly justified by the values of E and σ_R. However, in spite of the similar non-linear behaviour displayed at 600 and 1000 °C, the difference between the estimated and experimental values of ε_R is higher at 600 °C, which is attributed to the more marked softening behaviour at this temperature; in terms of non-linearity, the contribution made by the graphite and the organic binder decreases. At 1000 °C, B also has the least ability to deform.

The Young's modulus of B went down from 1000 to 1400 °C; this behaviour has been reported for aluminium-containing MgO–C materials (between 2.5 and 5.0 wt.%) bonding with resin [15] and the authors attribute this to the foam morphology of the spinel that replaces high stiffness Al_4C_3 in this temperature range. In reality, signs of spinel in B tested at 1400 °C could only be obtained by XRD since this phase is not detectable by SEM/EDS; these facts suggest that if spinel was indeed formed during the thermal treatment, the reaction was not general but occurred very locally (likely in the matrix). However, the presence of

Al_4C_3, SiC and other Si-containing crystalline or non-crystalline phases was clearly inferred by XRD and/or SEM. Based on the variation of the modulus E, neither the presence of this phase nor the local character of the spinel formed (no data regarding its morphology could be obtained) have a net beneficial effect on the stiffness of the refractory. Moreover, the decrease of the Young's modulus could indicate the glassy nature of the new Si-based phases. The increase in the true porosity is considered to be another contributing factor in the decrease of E in B. The small variation of the Young's modulus in pitch-bonded refractories is a combination of the spinel formation (the unique new phase confirmed by SEM and XRD, contributing to the increase of this parameter) and the variation of true porosity (lowering of E).

The fracture strength of A1 and A2 between 1000 and 1400 °C follows the same tendency as E and thus depends on the same factor: the strengthening effect of spinel (compared to that of Al_4C_3 [9] in any case) overcoming the increase in the porosity. Similarly, B exhibited an increase in σ_R in spite of the large increase in the total porosity, as was reported in similar resin-aluminium based materials and attributed to a crack sealing effect [15]. In this case, however, the presence of Si changes the scenario. On the one hand, a strengthening effect of new silicon-based phases or aluminium-based phases cannot be discarded. On the other hand, the presence of a silicate glassy phase which softens at high temperature could contribute to relieving the stress and increasing the mechanical strength.

At 1400 °C, the resin-bonded refractories' ability to deform matches to that of pitch-based A1 and A2 due to a considerable decrease of the Young's modulus of B. The σ_Y/σ_R ratio increases at 1400 °C, with values similar to those values at RT; the differences between the experimental fracture strain and σ_R/E ratio are also similar at both temperatures. In addition to the deformation mechanisms at work at 1000 °C, viscous plastic deformation due to the presence of low viscous phases (present as impurities or generated from silicon in the case of B) could also be a contributing factor. Moreover, the sealing of cracks and the filling of pores could contribute to reducing microcracking; similarly, the further oxidation of graphite and the transformation of the binder reduce the contribution of these phases to irreversible deformation.

As at RT, the mechanical parameters of the resin-bonded refractory (B) from 600 to 1400 °C remained higher than those of pitch bonded refractories, contrary to the results of Quintela et al. [41]. Taffin et al. [9] assert that a resin binder favours gaseous exchanges more than pitch, and this is the cause for the higher mechanical strength of the former. In agreement with this, a considerable increase in the porosity of B between 1000 and 1400 °C was observed. Moreover, the efficiency of the antioxidant depends on the ability of gaseous species to be formed throughout the material [34] extending the contact between the local zones where the additive acted [9]. In accordance with the literature, this is the case with Si above 1300 °C [9]. Both factors contribute to the higher values of σ_R and E for B with respect to the values for pitch-bonded materials (A1 and A2).

5. Conclusions

From a comprehensive analysis of the mechanical behaviour of pitch- and resin-bonded commercial MgO–C bricks, and based on a complete characterization of as-received and post-testing materials and previous well-documented studies, it can be asserted that:

- up to 1000 °C, the main microstructural changes involved the transformation of the organic binder (incomplete even at the highest temperature) and to a lesser extent, graphite oxidation (that is not completely avoided by the nitrogen flow); as a consequence, the mechanical behaviour of the two types of pitch-bonded bricks was quite similar, yet different compared to that of the resin-bonded refractory. In addition, the variation of Young's modulus was similar to that of fracture strength in every material,
- from 1000 °C to 1400 °C, the formation of new phases due to the reaction of antioxidants (Al and Si) became a determining factor affecting the mechanical behaviour of the studied bricks; in the case of pitch-bonded refractories, it was the formation of AlN at 1000 °C and spinel at higher temperatures that contributed to improving the mechanical properties; with respect to the resin-bonded material, the presence of Si-containing phases changes the material's response, and when the temperature increased to 1400 °C, mechanical strength increased whereas the Young modulus decreased, also due to increased porosity,
- resin-bonded material exhibited higher elastic modulus and greater mechanical strength than pitch-bonded refractories at both RT and at temperatures >1000 °C; this was mainly attributed to the type of binder and the presence of silicon in the first type of materials,
- the three bricks showed a quasi-brittle behaviour within the entire range of temperatures, much more so at 600 and 1000 °C due to an increase in microcracking; a softening behaviour was observed only in pitch-bonded materials at 600 °C,
- except at 1400 °C, the resin-bonded material showed the least ability to deform (higher fracture strain), mainly due to the type of organic binder; at this temperature, the three bricks have almost the same strain-to-fracture value.

From a mechanical point of view, resin-bonded refractory material seems to be better in terms of stiffness and load bearing capacity over the entire range of testing temperatures. However, this fact does not imply that this material performs better in service under thermomechanical loading conditions, since its low ability to deform and high stiffness make this material prone to suffer cracks, joint attack and thermal shock damage, at least up to 1000 °C. At 1400 °C, when its ability to deform is similar to those of the pitch-bonded materials, the refractory with resin as the organic binder is likely to perform best under mechanical and thermal stress.

The experimental data reported in this work and their interpretation in terms of mechanisms and microstructural changes are valuable information that not only contributes to

increasing the basic knowledge in this field of research, but also serves to help the users of these refractories, particularly for simulating stress fields in steelshop vessels and understanding the behaviour of the in-service materials. Besides the application of the mechanical properties obtained here in constitutive equations to describe the mechanical behaviour of the refractories, these parameters are also useful for the evaluation of other related behaviour of the materials such as the thermal shock resistance.

References

[1] C. Alvarez, E. Criado, C. Baudín, Refractarios de magnesia-grafito, Bol. Soc. Esp. Ceram. Vidr. 31 (1992) 397–405.

[2] R.E. Moore, The role of key components in the service life of magnesia–carbon–metal composite, Refractory Applications, 8–9, March 1997.

[3] J.E. Doig, Use of refractories magnesia linings in ladles and tundishes, Refractories Applications, 7–8, March 1998.

[4] R. Jhunjhunwala, M.M. Sahu, P.C. Padhi, S.P. Idicula, Advances in magnesia-carbon brick applications, in: Proceedings of UNITECR'93, São Paulo, Brazil, (1993), pp. 391–400.

[5] E.M.M. Ewais, Carbon based refractories, J. Ceram. Soc. Japan 112 (2004) 517–532.

[6] A.M. Fitchett, B. Wilshire, Mechanical properties of carbon-bearing magnesia-I. Pitch-bonded magnesia, Brit. Ceram. Trans. J. 83 (1984) 54–59.

[7] A.M. Fitchett, B. Wilshire, Mechanical properties of carbon-bearing magnesia-II. Pitch-bonded magnesia graphite, Brit. Ceram. Trans. J. 83 (1984) 59–62.

[8] A.M. Fitchett, B. Wilshire, Mechanical properties of carbon-bearing magnesia-III. Resin-bonded magnesia and magnesia-graphite, Brit. Ceram. Trans. J. 83 (1984) 73–76.

[9] C. Taffin, J. Poirier, The behaviour of metal additives in MgO–C and Al_2O_3–C refractories, Interceram 43 (1994) 354–358 [5]/458–460 [6].

[10] S.A. Franklin, B.J.S. Tucker, Hot strength and thermal shock resistance of magnesia-carbon refractories, Brit. Ceram. Trans. J. 94 (1995) 151–156.

[11] C. Baudín, C. Alvarez, Thermal history and mechanical behaviour for MgO–C refractories, in: Proceedings of UNITECR'95, Kyoto, Japan, (1995), pp. 84–91.

[12] C. Baudín, C. Alvarez, Influence of graphite-flake orientation on textural modifications of graphite-based refractories at high temperature, in: Proceedings of UNITECR'95, Kyoto, Japan, (1995), pp. 108–115.

[13] J.M. Robin, Y. Berthaud, N. Schmitt, J. Poirier, D. Themines, Thermo-mechanical behaviour of magnesia-carbon refractactories, Brit. Ceram. Trans. 97 (1998) 1–10.

[14] S. Uchida, K. Ichikawa, K. Niihara, High-temperature properties of unburned MgO–C bricks containing Al and Si powders, J. Am. Ceram. Soc. 81 (1998) 2910–2916.

[15] C. Baudín, C. Alvarez, R. Moore, Influence of chemical reactions in MgO-graphite refractories. I. Effect on texture and high-temperature mechanical properties, J. Am. Ceram. Soc. 82 (1999) 3529–3538.

[16] C. Baudín, C. Alvarez, R. Moore, Influence of chemical reactions in MgO-graphite refractories. II. Effect of aluminum and graphite contents in generic products, J. Am. Ceram. Soc. 82 (1999) 3539–3548.

[17] N. Schmitt, Y. Berthaud, J. Poirier, Tensile behaviour of magnesia carbon refractories, J. Eur. Ceram. Soc. 20 (2000) 2239–2248.

[18] C. Baudín, High temperature mechanical behaviour of magnesia graphite refractories, in: J. Bennett, J.D. Smith (Eds.), Fundamentals of Refractory Technology, Ceramic Transactions, vol. 125, The American Ceramic Society, Westerville, 2001, pp. 73–92.

[19] T. Suruga, E. Hatae, T. Hokii, K. Asano, Spalling resistance and physical behaviour of MgO–C refractories at high temperature, J. Tech. Assoc. Refr. 25 (2005) 128–131.

[20] C.G. Aneziris, D. Borozov, M. Hample, J. Suren, Flexibility of MgO–C refractories due to bending tests at room temperature and after thermal shock treatment, in: Proceedings of UNITECR'05, Orlando, USA, (2005), pp. 261–264.

[21] H. Jansen, C.G. Aneziris, M. Hampel, Y.W. Li, Microstructure and mechanical behaviour of magnesia-carbon bricks bonded by catalytically activated resins, in: Proceedings of the UNITECR'07, Dresden, Germany, (2007), pp. 38–41.

[22] DIN EN 993-1, Method of Test for Dense Shaped Refractory Products. Determination of Bulk Density, Apparent Porosity and True Porosity, 1995 (DIN 51056).

[23] ASTM 329-88, Standard Test Method for Specific Gravity of Fired Ceramic Whiteware Materials, 1994.

[24] V. Muñoz, G.A., Rohr, A.L., Cavalieri, A.G. Tomba Martinez, Experimental methodology for mechanical evaluation of oxide-carbon refractories by strain measurement, J. Test. Eval., doi:10.1520/JTE103455, in press.

[25] B. Rand, B. McEnaney, Carbon binders from polymeric resins and pitch Part I –pyrolisis behaviour and structure of the carbons, Brit. Ceram. Trans. J. 84 (1985) 165–175.

[26] W. Vieira, B. Rand, Microstructure development in pitch-containing alumina-carbon refractory composites, in: Proceedings of UNITECR'97, New Orleans, USA, (1997), pp. 851–859.

[27] A. Yamaguchi, Application of thermochemistry to refractories, in: J. Bennett, J.D. Smith (Eds.), Fundamentals of Refractory Technology, vol. 125, Ceramic Transactions, The American Ceramic Society, 2001, pp. 157–170.

[28] M. Bavand-Vandchali, F. Golestani-Fard, H. Sarpoolaky, H.R. Rezai, C.G. Aneziris, The influence of *in situ* spinel formation on microstructure and phase evolution of MgO–C refractories, J. Eur. Ceram. Soc. 28 (2008) 563–569.

[29] A. Gardziella, J. Suren, M. Belsue, Carbon form phenolic resins: carbon yield and volatile componentes – recent studies, Interceram 41 (1992) 461–467.

[30] K. Kanno, N. Koike, Y. Korai, I. Mochida, M. Komatsu, Mesophase pitch and phenolic resin blends as binders for magnesia-graphited bricks, Carbon 37 (1999) 195–201.

[31] K. Takeuchi, S. Yoshida, S. Tsuboi, Gas phase oxidation of MgO–C bricks, J. Tech. Assoc. Refract. Jpn. 23 (2003) 276–279.

[32] G. Buchebner, R. Nauboeck, S. Grassegger, Carbon-bonding – a new milestone on low emission magnesia-carbon bricks, in: Proceedings of UNITECR'01, Cancun, Mexico, 2001.

[33] G. Liu, H. Li, B. Yang, J. Wang, X. Wang, The influence of heat-treating atmosphere on Al_2O_3–C material with Al addition, in: Proceedings of UNITECR'05, Orlando, USA, 2005.

[34] M. Rigaud, P. Bombard, X. Li, B. Guéroult, Phase evolution in various carbon-bonded basic refractories, in: Proceedings of UNTECR'93, São Paulo, Brazil, (1993), pp. 360–371.

[35] B.H. Baker, B. Brezny, Dense zone formation in magnesia-graphite refractories, in: Proceedings of UNITECR'91, Aachen, Alemania, (1991), pp. 168–172.

[36] H. Baudson, F. Debucquoy, M. Huger, C. Gault, M. Rigaud, Ultrasonic measurement of Young's modulus MgO/C refractories at high temperature, J. Eur. Ceram. Soc. 19 (1999) 1895–1901.

[37] W.E. Lee, W.M. Rainforth, Ceramic Microstructures, Chapman & Hall, 1994 471pp.

[38] A. Yoshida, On the present status of seawater magnesia manufacturing, J. Tech. Assoc. Refr. 25 (2005) 89–99.

[39] B. McEnaney, B. Rand, Carbon binders from polymer resins and pitch. Part II – structure and properties of carbon, Brit. Ceram. Trans. J. 84 (1985) 193–198.

[40] A. Figueiredo, N. Bellandi, A. Vanola, L. Zamboni, Technological evolution of magnesia-carbon bricks for steel ladles in Argentina, Iron Steel Technol. 1 (2004) 42–47.

[41] M.A. Quintela, F.D. Santos, C.A. Pessoa, J. de Anchieta Rodriguez, V.C. Pandolfelli, MgO–C refractories for steel ladles salg line, Refractories Application and News (Septembre/October 2006) 15–19.

[42] G. Bhatia, R.K. Aggrwal, M. Malik, O.P. Bahl, Conversion of phenol formaldehyde resin to glass-like carbon, J. Mater. Sci. 19 (1984) 1022–1028.